The Plant Cell, Vol. 16, 2586–2600, October 2004, www.plantcell.org © 2004 American Society of Plant Biologists

# HANABA TARANU Is a GATA Transcription Factor That Regulates Shoot Apical Meristem and Flower Development in Arabidopsis [W]

**Yuanxiang Zhao, Leonard Medrano,[1,2] Kazuaki Ohashi,[2,3] Jennifer C. Fletcher,[4] Hao Yu,[5] Hajime Sakai,[6] and Elliot M. Meyerowitz[7]**

Division of Biology, California Institute of Technology, Pasadena, California 91125

**We have isolated a new mutant, *hanaba taranu* (*han*), which affects both flower and shoot apical meristem (SAM) development in *Arabidopsis thaliana*. Mutants have fused sepals and reduced organ numbers in all four whorls, especially in the 2nd (petal) and 3rd (stamen) whorls. *han* meristems can become flatter or smaller than in the wild type. *HAN* encodes a GATA-3–like transcription factor with a single zinc finger domain. *HAN* is transcribed at the boundaries between the meristem and its newly initiated organ primordia and at the boundaries between different floral whorls. It is also expressed in vascular tissues, developing ovules and stamens, and in the embryo. *han* interacts strongly with *clavata* (*clv*) mutations (*clv1*, *clv2*, and *clv3*), resulting in highly fasciated SAMs, and we find that *WUS* expression is altered in *han* mutants from early embryogenesis. In addition, *HAN* is ectopically expressed both in *clv1* and *clv3* mutants. We propose that HAN is normally required for establishing organ boundaries in shoots and flowers and for controlling the number and position of *WUS*-expressing cells. Ectopic *HAN* expression causes growth retardation, aberrant cell division patterns, and loss of meristem activity, suggesting that HAN is involved in controlling cell proliferation and differentiation.**

## INTRODUCTION

During the reproductive growth phase of *Arabidopsis thaliana*, flowers arise in a spiral phyllotaxis from the flanks of the shoot apical meristem (SAM), which is located at the tip of the stem and encompasses a stem cell population whose descendants essentially give rise to all of the aerial parts of the plant. The SAM can be divided into three zones: the central zone, which is composed of a small number of slowly dividing stem cells at the meristem apex, the rib meristem zone, which lies underneath the central zone and gives rise to the pith and vascular structure of the stem, and the peripheral zone, which surrounds the central zone and provides founder cells for the formation of new leaves and flowers (reviewed in Fletcher and Meyerowitz, 2000). Floral primordia originate as a buttress of undifferentiated cells (the floral meristem) growing at the peripheral zone of the SAM, which soon separates itself from the SAM (only connects to the stem through its peduncle) and sequentially gives rise to the sepals, the petals, and the stamens. Eventually the remaining inner floral meristem cells differentiate into two congenitally fused carpels (Smyth et al., 1990).

Two major pathways, the WUSCHEL (WUS)–CLAVATA (CLV) pathway and the SHOOT MERISTEMLESS (STM) pathway, have been characterized as pivotal for meristem establishment and maintenance. Both *wus* and *stm* mutants fail to initiate an embryonic SAM and have premature termination of adventitious shoot and floral meristems (Clark et al., 1996; Laux et al., 1996; Long et al., 1996). *WUS* encodes a homeodomain protein that is expressed near the boundary of the central zone and rib meristem in shoot and floral meristems and functions to promote meristem activity (Mayer et al., 1998). The *clv* mutations (*clv1*, *clv2*, and *clv3*) affect both SAM and floral meristem development, resulting in enlarged shoot apical and floral meristems as well as increased floral organ numbers (Clark et al., 1996, 1997; Kayes and Clark, 1998). *CLV3* is normally expressed in the central zone, overlying the *WUS* domain (Fletcher et al., 1999), whereas *CLV1* is expressed in the rib meristem zone, embracing the *WUS* domain basally and laterally (Clark et al., 1997). It has been suggested that CLV3, a secreted small protein (Fletcher et al., 1999; Rojo et al., 2002), interacts with the CLV1/CLV2 Leu-rich repeat receptor proteins as a ligand/receptor complex to activate a signal transduction cascade that limits *WUS* expression (Fletcher et al., 1999; Brand et al., 2000; Schoof et al., 2000). In the absence of CLV activity, WUS activity increases and causes accumulation of stem cells and thereby an enlarged, fasciated meristem.

[1] Current address: Ceres Inc., 1535 Rancho Conejo Blvd., Thousand Oaks, CA 91320.
[2] These authors contributed equally to the work.
[3] Current address: Laboratory of Molecular and Biochemical Toxicology, Graduate School of Pharmaceutical Sciences, Tohoku University, Japan.
[4] Current address: Plant Gene Expression Center, USDA/University of California, Berkeley, CA 94710.
[5] Current address: Department of Biological Sciences, National University of Singapore, 117543 Singapore.
[6] Current address: DuPont Crop Genetics, Experimental Station E353, Wilmington, DE 19880.
[7] To whom correspondence should be addressed. E-mail meyerow@caltech.edu; fax 626-449-0756.
The author responsible for distribution of materials integral to the findings presented in this article in accordance with the policy described in the Instructions for Authors (www.plantcell.org) is: Yuanxiang Zhao (zhaoyx@caltech.edu).
[W] Online version contains Web-only data.
Article, publication date, and citation information can be found at www.plantcell.org/cgi/doi/10.1105/tpc.104.024869.

Conversely, it has been shown that ectopic *WUS* expression can induce ectopic *CLV3* expression (Schoof et al., 2000). It has been proposed, therefore, that WUS regulates its activity so as to control SAM size by employing a negative feedback system involving the CLV proteins. *STM* encodes a member of the class 1 *KNOX* family of homeodomain proteins (Long et al., 1996). *STM* is expressed throughout the SAM where it appears to act through downregulating the *ASYMMETRIC LEAVES* genes (*AS1* and *AS2*). Loss of AS1 activity restores meristem function to *stm* mutants by derepressing the activities of other *KNOX* class genes, such as *KNAT1* (also named *BREVIPEDICELLUS*; Venglat et al., 2002) and *KNAT2* (Byrne et al., 2000). More recently it has been shown that the STM and WUS pathways can act together to confer ectopic meristematic cell fate (Gallois et al., 2002; Lenhard et al., 2002).

Although much is known about genetic regulatory pathways within the SAM, little is known about the interactions between meristematic cells and their neighboring differentiating cells. Nevertheless, molecules coupling differentiating cells with meristem development have been uncovered in recent years. In *Petunia hybrida*, *Hairy Meristem* (*HAM*) encodes a GRAS family putative transcription factor that is expressed in provascular tissue, but *ham* mutations result in early termination of SAM activity. Hence, HAM may represent an extrinsic antidifferentiation factor that is required to maintain stem cells in the SAM (Stuurman et al., 2002). Additionally, lateral organ polarity genes, such as *Antirrhinum majus PHANTASTICA* and Arabidopsis *PHABULOSA*, also appear to have positive effects on the formation and maintenance of apical meristems (McConnell and Barton, 1998; Waites et al., 1998). Furthermore, members of the NAC-domain gene family expressed at the boundaries of meristems and primordia, including the Petunia *NO APICAL MERISTEM* (Souer et al., 1996), the Antirrhinum *CUPULIFORMIS* (Weir et al., 2004), and the Arabidopsis *CUP-SHAPED COTYLEDON* genes *CUC1*, *CUC2*, and *CUC3* (Aida et al., 1999; Takada et al., 2001; Vroemen et al., 2003), regulate SAM development as well. In this report, we describe a new gene in Arabidopsis, *HANABA TARANU* (*HAN*; meaning fewer floral leaves in Japanese), that is required for normal flower and SAM development. This gene is expressed in the provascular tissues during embryogenesis and later is expressed at the boundary tissues between meristems and initiating organ primordia as well as in the vascular tissues. We demonstrate that *han* mutations interact strongly with *clv* mutations and that HAN is required for normal cell division and positioning of *WUS*-expressing cells in the SAM, suggesting that HAN also represents one of the extrinsic molecules linking the more mature boundary and vascular cells with SAM activities.

## RESULTS

### *han* Mutant Phenotypes and *HAN* Cloning

Four different *han* mutant alleles (*han-1* to *han-4*) were isolated in three different mutagenesis screens in Arabidopsis. *han-2* was isolated in an ethyl methanesulfonate mutagenesis screen, and the *han-1*, *han-3*, and *han-4* alleles were generated in two separate *Agrobacterium tumefaciens*–mediated *T-DNA* screens (see Methods). All *han* mutants have similar flower defects, including fused sepals, reduced numbers of petals and stamens, and, sometimes, unfused carpels. Phenotypically *han-2* is the weakest allele, and *han-3* is the strongest, whereas *han-4* and *han-1* have similar, intermediate expressivity. Mutants homozygous for *han-3*, unlike lines homozygous for the other alleles, have fasciated SAMs. In addition, the *han-3* allele shows slight semidominance, whereas the other *han* mutations are fully recessive. We will focus on the recessive mutations in this report. The majority of *han-2* mutant flowers have two to four sepals (sepals fused together are counted as 1) in the 1st whorl, one or two organs in the 2nd whorl (including petals as well as filamentous structures), four or five stamens (including filaments lacking anthers) in the 3rd whorl, and two asymmetric carpels in the 4th whorl (Table 1, Figures 1B to 1E). Malformed organs observed include bifid stamens with two stalks fused partially or completely along their length but with anthers separated (Figure 1C, arrow), filamentous structures between whorls (Figure 1D), and stamens with abnormal anthers. In >50% (31/54) of the cases, the valves of the two fused carpels are not symmetrical, with one shorter than the other at the basal region (Figure 1E, arrow). At a much lower frequency (4/54), extra tissue is formed apically (Figure 1E, arrowhead). *han-2* homozygous plants are partially fertile. *han-1* flowers have stronger defects in all whorls when compared with *han-2* flowers. In approximately half of *han-1* flowers, all of the sepals are either partially or completely fused (Table 1, Figures 1F to 1H). Mature petals are rare and only appear in a few early flowers. The majority of *han-1* flowers lack second whorl organs. In the third whorl, organ numbers are generally decreased to

**Table 1.** *han* Flower Phenotypes Summary

| Organ Number | Sepal | | | | | | Petal | | | | | Stamen | | | | | | | Carpel | | |
|---|---|---|---|---|---|---|---|---|---|---|---|---|---|---|---|---|---|---|---|---|---|
| Flower Number | 0 | 1 | 2 | 3 | 4 | 5 | 0 | 1 | 2 | 3 | 4 | 0 | 1 | 2 | 3 | 4 | 5 | 6 | 2 | Fused | Unfused |
| *han-2* | 0 | 4 | 27 | 57 | 21 | 1 | 13 | 31 | 40 | 23 | 3 | 0 | 0 | 0 | 6 | 40 | 55 | 9 | 49[b] | 54 | 0 |
| 110[a],[b] | | | | | | | | (4) | (10) | (13) | (2) | | | | | (4) | (6) | (1) | | | |
| *han-1* | 0 | 53 | 37 | 13 | 4 | 0 | 77 | 24 | 4 | 2 | 0 | 0 | 8 | 12 | 37 | 32 | 16 | 1 | 107 | 91 | 16 |
| 107[a] | | | | | | | | (6) | | (3) | | | (3) | (11) | (77) | (90) | (62) | (4) | | | |

The numbers in parentheses represent the total number of filamentous structures in all flowers of each category.

[a] Total number of flowers examined.

[b] Only 54 flowers were examined for carpel number and fusion defects. Of the 54, 49 had two carpels, 1 had a single carpel, and 4 had extra carpel tissues positioned apically.

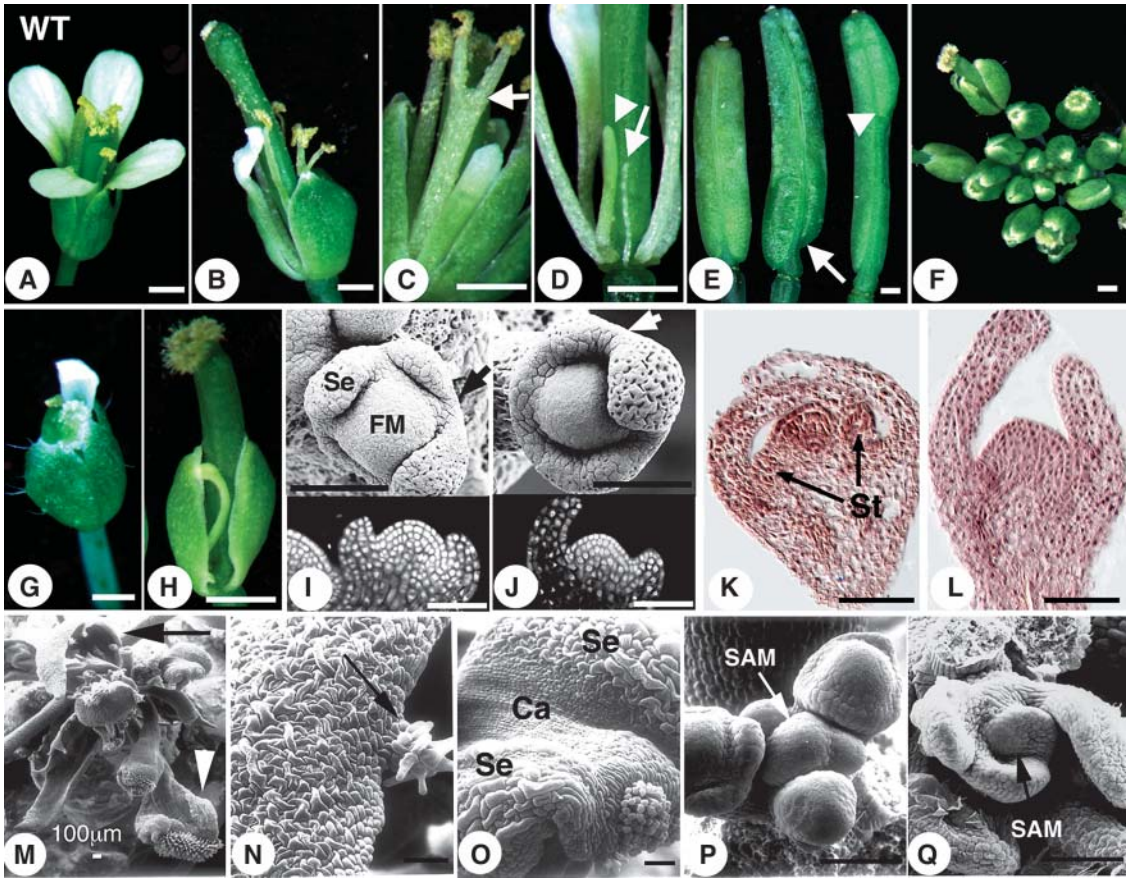


**Figure 1.** *han* Mutant Flower and Floral Meristem Phenotypes.

**(A)** A wild-type flower.
**(B)** to **(E)** *han-2* homozygotes.
**(F)** to **(H)** *han-1* homozygotes.
**(B)** A *han-2* flower.
**(C)** The arrow points to the fusion of two stamens.
**(D)** Filamentous structures in place of a petal or a stamen are indicated by the arrow and arrowhead, respectively. Sepals were removed.
**(E)** Carpel defects include asymmetric silique valves (arrow) and extra carpel tissue positioned at the apical region of the silique (arrowhead). Siliques shown are not age-matched.
**(F)** A *han-1* inflorescence.
**(G)** An early-arising *han-1* flower.
**(H)** A flower with sepals all fused into an open semicircle.
**(I)** A wild-type stage 3 flower. Se, sepal; FM, floral meristem.
**(J)** A *han-1* stage 3 flower (because *han* floral meristem development is generally delayed, floral stage is determined based on sepal size).
**(K)** A wild-type stage 6 flower. St, stamens.
**(L)** A *han-1* stage 6 flower.
**(M)** A *han-1* inflorescence at late stage. The black arrow points to a carpelloid sepal, and the white arrowhead points to a sepalloid carpel.
**(N)** An enlarged view of the carpelloid sepal indicated in **(M)**. Arrow points to stigmatic papillae at the edge of the sepal.
**(O)** An enlarged view of the sepal (Se) and carpel (Ca) fusion structure in **(M)**.
**(P)** A wild-type SAM.
**(Q)** A *han-1* mutant SAM.
Bars in **(A)** to **(H)** = 0.5 mm; bars in **(I)** to **(Q)** = 50 μm (unless indicated otherwise).

three or four, and stamens with normal morphology are rare. The frequency of filamentous structures occupying stamen positions in *han-1* flowers is much higher than in *han-2* flowers. *han-1* homozygous plants have extremely low fertility. Consistent with their reduced floral organ numbers and sizes, *han-1* mutants have smaller floral meristems than the wild type, as shown for a stage 3 flower in Figure 1J (arrow points to an area of congenital sepal fusion). In addition, inner whorl organ primordia either fail to develop or are delayed in appearance compared with the wild type in stage 6 flowers (Figures 1K and 1L).

Vegetative growth and inflorescence structure of *han* mutants appears fairly normal. However, in some of the *han-1* and *han-4* plants, flowers that arise toward the end of the reproductive stage are morphologically more deformed than early flowers, composed either of carpels alone (sometimes subtended by leaf/sepal-like structures), carpelloid sepal/leaf-like structures (Figures 1M and 1N, arrows), or chimeric organs with carpelloid character (Figures 1M, arrowhead, and 1O). In addition, later-arising flowers fail to originate in a typical phyllotactic spiral. Perturbed floral phyllotaxy generally reflects a SAM defect. To determine if such a defect is visible in *han-1* mutants, both early (postembryonic day 30) and late stage (after postembryonic day 40) inflorescence SAMs were examined using scanning electron microscopy. Early stage *han* SAMs are normal compared with the wild type, as also confirmed by confocal laser scanning microscopy (data not shown). However, for the late stage *han* inflorescences, five out of eight SAMs appeared flattened instead of dome-shaped as in the wild type (Figures 1P and 1Q) and in some cases appeared smaller and less distinct from the surrounding initiating organ primordia. In the flattened SAMs, early stage floral organ primordia were not the usual hemispherical masses of undifferentiated cells but were ridge-shaped. This indicates that there is a gradual transition toward an aberrant SAM morphology in *han* mutants during reproductive development.

The *HAN* gene was cloned by both positional mapping of the *han-1* allele and by *T-DNA* tagging of the *han-4* allele. *HAN* is located on chromosome 3 (At3g50870), and its full-length *cDNA* was isolated from a flower-specific λ*cDNA* library. The protein sequence deduced from the open reading frame consists of 295 amino acids, encoded by two exons, and resembles a GATA-3–like protein with a single zinc finger motif (C-$X_2$-C-$X_{18}$-C-$X_2$-C) (Figure 2). In addition, there is a stretch of 14 amino acids N-terminal to the zinc finger that appears highly conserved among some plant GATA transcription factors. The *han-1* mutation results in a complete deletion of the gene, starting from 709 bp upstream of the translation initiation codon and ending at 1298 bp downstream of the stop codon. The mutation in *han-2* results in a single amino acid change at position 179, Gly (GGC) to Ser (AGC). The mutation in *han-4* is caused by the insertion of at least two copies of a *T-DNA* sequence into the intron at 112 bp, followed by a deletion of 20 bp. Both a 9- and 6-kb genomic fragment spanning the *HAN* gene fully rescues the *han* phenotypes (data not shown). Database searches identified 25 putative *GATA* genes in the Arabidopsis genome, among which are two close HAN relatives, located on chromosomes 2 and 4 (At2g18380 and At4g36620), and here named HANL1 and HANL2. The *HAN* gene shares 46 and 50% sequence similarity to its two close homologs *HANL1* and *HANL2*, respectively.

### *HAN* Expression

The *HAN* expression pattern was examined by in situ hybridization using a full-length *cDNA* probe and a *HAN*-specific 5′-cDNA probe, both of which are specific to HAN (see Methods) and which gave the same results. *HAN* is expressed in vegetative and inflorescence SAMs, axillary SAMs, floral meristems, developing ovules and stamens, vascular tissues, and in the embryo. In the developing axillary SAM, it is expressed at the boundary between nascent axillary meristems and the adaxial side of leaves (Figure 3A, a, arrows). Expression in all mature SAMs is similar, located at the boundaries between the central SAM and the initiating organ primordia, as well as between the neighboring initiating organ primordia (Figures 3A, b and c, and 3B).

Expression in the floral meristem reiterates the pattern seen in the SAM, with strong expression at the boundaries between the meristematic dome and the initiating floral organ primordia, and also at the boundaries between the primordia of different whorls (Figure 3A, d). Expression at the boundaries attenuates as the organ primordia grow apart. In stage 5 flowers, expression remains at the boundary between the central meristematic cells and differentiating stamen primordia (data not shown). In stage 6 flowers, expression is the strongest at the medial ridge region of the carpel (Figure 3A, e). In the developing ovule, *HAN* is expressed in the inner and outer integuments, with signal absent from the nucellus (Figure 3A, f and g). In all of the aerial tissues examined, including flowers, *HAN* is expressed strongly in cell types associated with the phloem tissues (arrows in Figure 3A, f and g). It is expressed strongly in the developing anthers in as

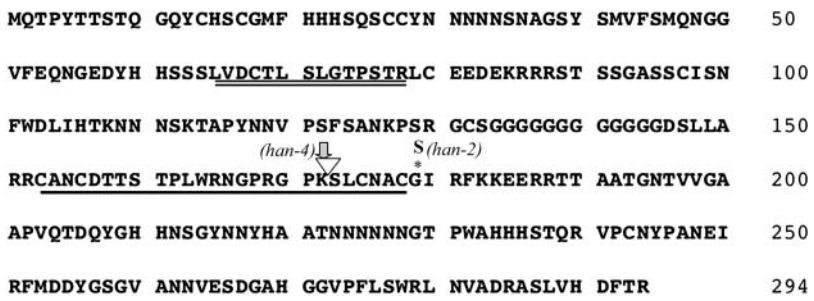


**Figure 2.** Protein and Gene Structure.

The HAN protein sequence deduced from the open reading frame of the full-length *HAN cDNA*. The position of the intron is indicated by the open triangle; a 14–amino acid domain that is highly conserved among some plant GATA factors is underlined twice; the zinc finger domain is underlined once. The mutation in *han-1* results in deletion of the whole gene. The mutation in *han-2* changes a Gly (GGC) to a Ser (AGC) at amino acid position 179 (asterisk). The mutation in *han-4* results from a *T-DNA* insertion within the intron (arrow). The 5′ junction sequence is flanked by the *Bar* gene in the *T-DNA*, whereas the 3′ is flanked by the 4× *35S* promoter in the *T-DNA* (near the right border).

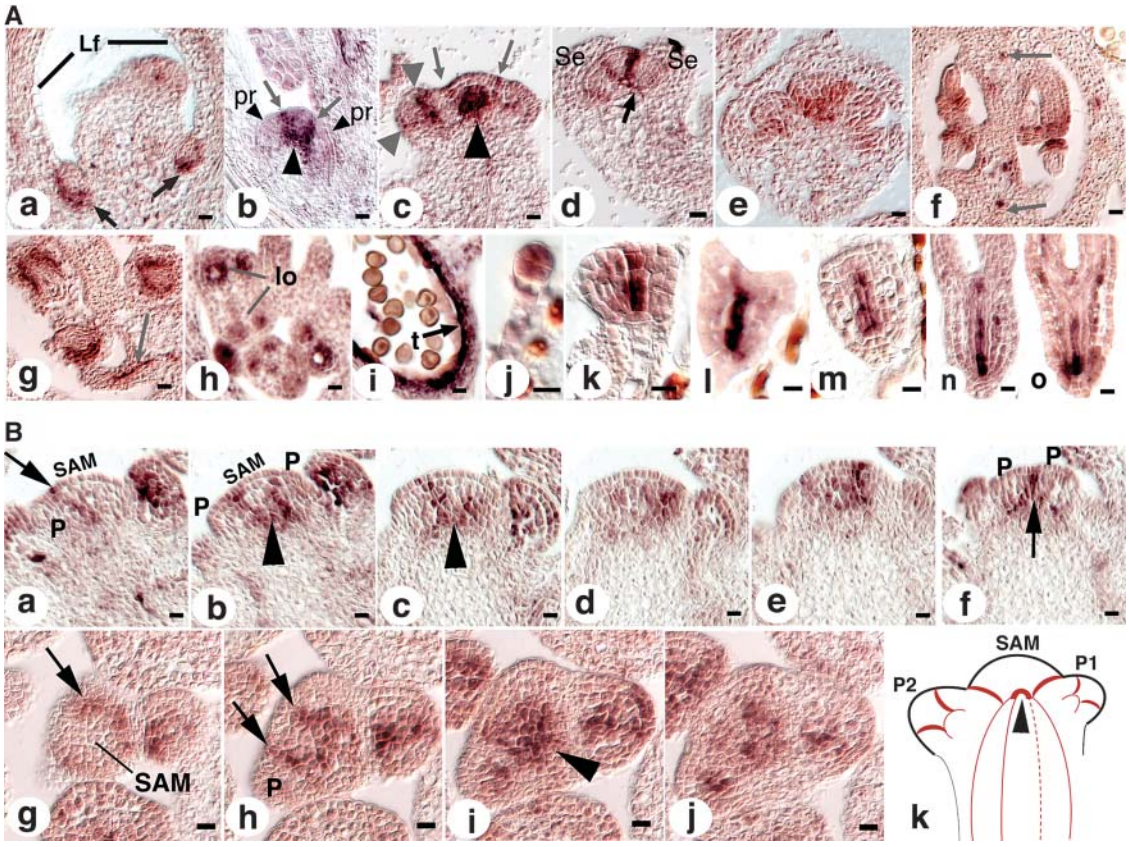


**Figure 3.** *HAN* Expression Pattern.

**(A)** Budding axillary SAMs are shown in (a). Arrows point to the expression domains of *HAN* at the boundaries between the SAM and the adaxial sides of leaves. Lf, leaf. (b) Older axillary SAM. Arrows point to the expression domains of *HAN* at the boundaries between the SAM and the newly initiated organ primordia (pr, small arrowheads). Large arrowhead indicates the junction of the *HAN* expression domain in the SAM and its vascular expression in the stem. (c) Inflorescence SAM. Arrows point to two stripes of *HAN* expression at the boundaries between the SAM and newly initiated floral primordia. Small arrowheads indicate *HAN* expression in a stage 2 flower at the boundaries between the floral meristem and the soon-to-be-specified sepal primordia. Large arrowheads point to the junction of the *HAN* expression domain in the SAM and in the stem (note that the angle of this section is tilted toward the reader, and the domain indicated by the large arrow includes some of the expression of *HAN* between the SAM and a primordium pointing toward the reader). (d) Stage 5 flower. Arrow points to the connection arch of *HAN* expression in the floral meristem and its expression in the peduncle vascular tissue. Se, sepal. (e) Expression in the lateral and basal regions of carpel primordia in a stage 6 flower. (f) Early stage 12 ovary (cross section). *HAN* is expressed in initiating inner and outer integuments as well as in the vascular tissue (arrows). (g) Expression in integuments continues in the stage 13 ovary. Arrow points to expression in funiculus vascular tissue. (h) *HAN* expression in the stamens of a stage 8 flower. lo, locule. (i) *HAN* expression persists in the tapetum cell layer until it has degenerated and is absent in mature haploid pollen. t, tapetum. (j) Eight-cell stage embryo. *HAN* is expressed in all cells of the embryo proper. (k and l) Globular and transition stage embryos. *HAN* is expressed in the center files of cells. (m and n) Heart and torpedo stage embryos. *HAN* expression remains in the center cells destined to be provascular tissues. (o) Late torpedo stage. Bars = 10 μm.
**(B)** Expression in SAM in serial longitudinal (a to f) and cross sections (g to j). Arrows point to expression at the boundaries between the SAM and new organ primordia as well as between organ primordia. Expression of *HAN* in the SAM merges with its expression in the vascular strands in the stem (arrowheads) as illustrated in (k). In (k), red lines represent the expression domains of *HAN* in the SAM, stem, and developing organ primordia (P1 and P2). Arrowhead corresponds to the regions indicated by large arrowheads in Figure 3A (b and c). P, primordium. Bars = 10 μm.

early as stage 8 flowers when locules are initiated, in the tapetum cell layer, as well as the microsporocytes (Figure 3A, h). Expression persists until the tapetum layer degenerates and haploid pollen is mature (Figure 3A, i). Expression of *HAN* in the embryo is detected uniformly in the embryo proper of the eight-cell stage embryo (Figure 3A, j). It is then concentrated in the center cells of the embryo and absent from the epidermal cell layer at the globular stage (Figure 3A, k). This expression pattern persists in the center four files of cells; expression is not observed in the outermost two apical layers through the transition and late heart stages (Figure 3A, l to n). In the torpedo stage embryo, expression is detected in all provascular tissues (Figure 3A, o).

### Genetic Interactions of *han* with Mutations Affecting Flower Development

Double mutants of *han-1* with the floral organ identity mutations *apetala 3*, *pistillata*, and *agamous* are generally additive (data not

shown). To determine if floral organ identity genes are affected in their expression in *han* mutants, *AP1* and *AP3* expression was examined in *han-1* flowers. For both genes, expression was detected in the mutant in correct spatial and temporal patterns, but signal intensity was relatively low (data not shown). The lower expression intensity is potentially because of a smaller number of floral organ cells in *han* mutants. This indicates that the floral organ identity genes act independently of *HAN* in controlling flower development.

Double mutants of *han* and *clv* (including *clv1*, *clv2*, and *clv3*) or *han* and *wus-1* were generated. Any combination of *han/clv* double mutants results in increased inflorescence fasciation and increased floral abnormalities as compared with either single mutant. Among all *clv* mutants, the *clv3-2* mutants show the strongest phenotype with regards to SAM fasciation and increased floral organ numbers in all four whorls (Figures 4A and 4B). Interactions between *han-2* and *clv3-2* or *han-1* and *clv3-2* make for very short plants with fasciated stems thicker than those of *clv3-2* single mutants. Early-arising flowers have elongated pedicels (Figure 4C, arrowhead) and are composed only of reduced sepals (or sepal-like tissue) and carpels, which are sometimes indeterminate and generate many sepal- or leaf-like structures from the base, or on top of an undifferentiated mass within the carpel valves (Figure 4D). Later-arising organs are either filamentous or are bracts tipped with stigmatic tissue, arising simultaneously in large numbers (Figure 4C, arrow). The *han-2 clv1-1* double mutants have either a fairly normal stem or are shorter and more fasciated than *clv1-1* and accumulate numerous flowers at the top of the inflorescence SAM (Figure 4E). These double mutant flowers generally have reduced organ numbers in the outer three whorls compared with *han-2* mutant flowers (Figure 4F). The *han-2 clv2-1* double mutants either appear similar to *han-2 clv1-1* mutants or lack primary shoot dominance and have several unfasciated stems terminating in a ball of carpelloid structures (Figure 4G). *han-1 clv1-1* and *han-1 clv2-1* double mutants produce inflorescences more fasciated than *clv* single mutants, with flowers for the most part composed only of sepals and sometimes unfused carpels (Figure 4H). The phenotypes of *han-4 clv* double mutants are similar to those of *han-1 clv* double mutants.

*han-1 wus-1* double mutants resemble *wus-1* single mutants, except that they appear darker green in color and have many more radial-shaped leaf-like structures (with trichomes) arising from the leaf axils (Figure 4J). No flowers were observed in *han-1 wus-1* double mutants (three plants). The *han-1/han-1 wus-1/+* mutants are phenotypically similar to *han-1* single mutants (data not shown). We further compared the number of floral organs present in *han-1/+ wus-1/wus-1* flowers versus *wus-1/wus-1* flowers. The former have an average of 3.2 ($\pm$1.1) sepals, 1.5 ($\pm$1.3) petals, and 0.5 ($\pm$0.9) stamens (including in 27% of cases filamentous structures) in 22 flowers counted, whereas the latter has an average of 3.9 ($\pm$1.0) sepals, 3.9 ($\pm$0.6) petals, and 1.1 ($\pm$0.3) stamens (no filamentous structures) of 10 flowers counted. The P value for each organ type difference based on an unpaired Student's *t* test is smaller than 0.05, suggesting that the difference is significant. This suggests that whereas *wus* is epistatic to

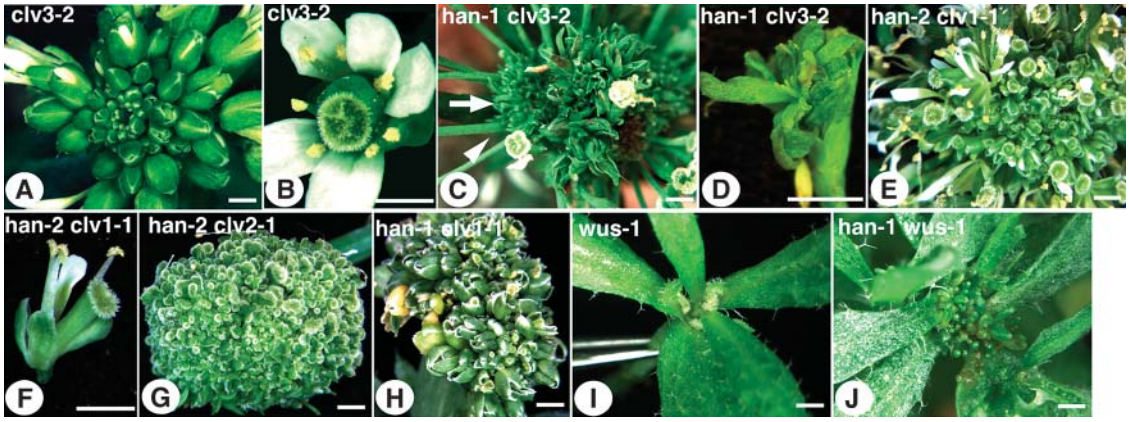


**Figure 4.** Genetic Interactions of *han* and *clv*.

**(A)** *clv3-2* inflorescence, top view.
**(B)** *clv3-2* flower, top view.
**(C)** *han-1 clv3-2* double mutant inflorescence. Arrowhead points to an early-arising flower with long peduncle, and arrow points to late-arising bract-like or filamentous organs.
**(D)** *han-1 clv3-2* double mutant flower.
**(E)** *han-2 clv1-1* double mutant inflorescence.
**(F)** *han-2 clv1-1* double mutant flower.
**(G)** *han-2 clv2-1* double mutant inflorescence.
**(H)** *han-1 clv1-1* double mutant inflorescence.
**(I)** *wus-1* single mutant axillary shoot.
**(J)** *han-1 wus-1* double mutant axillary shoot.
Bars = 1 mm.

*han* in overall development, flower development in *wus* mutants relies on HAN activity in a dose-dependent manner.

### HAN Regulates *WUS*-Expressing Cells

*WUS* serves as the earliest known marker for SAM development. It is detected in the inner two cells at the apical region of the 16-cell stage embryos, and its expression domain enlarges in embryonic and postembryonic SAMs of *clv* mutants (Mayer et al., 1998; Brand et al., 2000; Schoof et al., 2000). Because *han* mutations strongly enhance *clv* SAM phenotypes, we examined *WUS* expression in both *han* single mutants and *han clv* double mutants. In wild-type inflorescence meristems and floral meristems, *WUS* is expressed in the central region of the SAM, beneath the outermost two or three cell layers (Figures 5A and 5B). Expression in the floral meristem attenuates after stage 3 and is no longer detectable after stage 6. *WUS* expression in *clv3-2* inflorescence and floral meristems expands outward along the fasciated meristems and upward into the L2 layer (Figures 5C and 5D). In most of *han-1* and *han-4* inflorescences, whether in early or late stages of development, the *WUS* expression domain appears diffuse compared with the wild type, with a few central cells showing the strongest expression and surrounding cells showing weaker expression (Figures 5E and 5G). In the floral meristem, *WUS* expression is clearly shifted to include the L2 and L1 layers (Figures 5F and 5H). As in the SAM, the signal appears diffuse, with the border between the *WUS*-expressing cells and the surrounding cells not as sharp as is observed in the wild type or in *clv3-2* mutants. In some *han* meristems, however, *WUS* expression appears comparable to that in the wild type (see Supplemental Figure 1 online and Discussion).

In *han-1 clv3-2* double mutants, the inflorescence SAM region is expanded compared with *clv3-2* single mutants (Figures 5K and 5L). In contrast with its expression pattern in the *clv3-2* single mutant, *WUS* expression in the SAMs of the double mutants is concentrated in the L2 layer cells (Figure 5I), and in the floral meristems, expression extends upward into the epidermal cell layer in some cases (Figure 5J). Ectopic expression of *WUS* in *han-1* or *han-4* flowers all along the inflorescences is also observed, appearing in undifferentiated cells in late stage flowers and in the sepals, which in some cases are clearly carpelloid as they produce *WUS*-expressing ovules (data not shown).

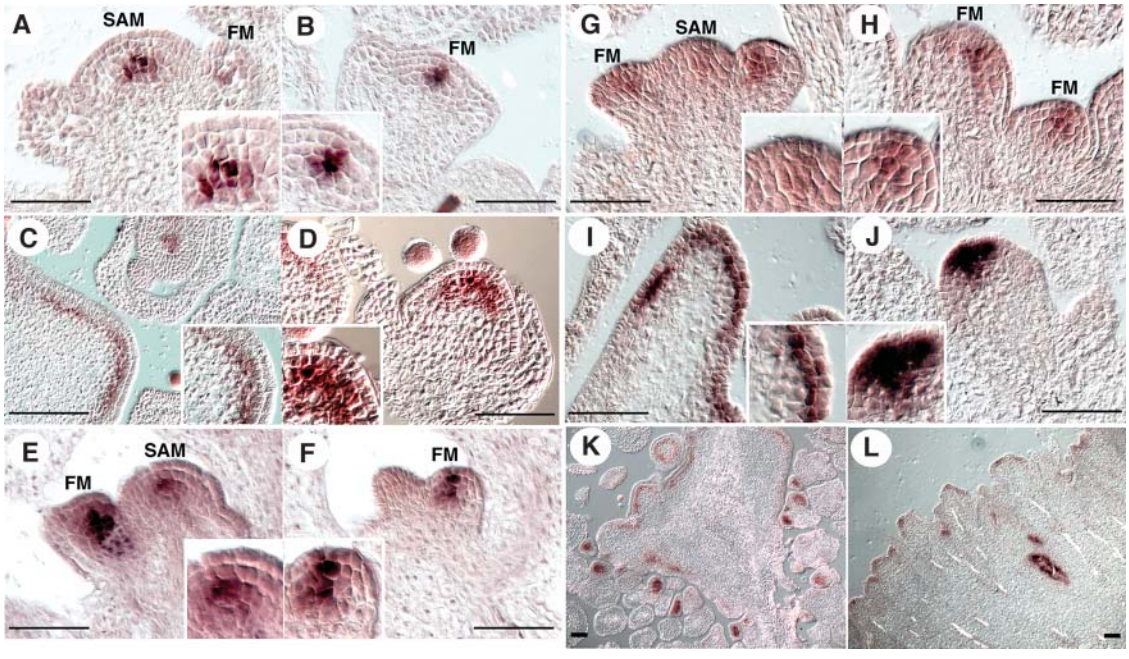


**Figure 5.** HAN Regulates *WUS*-Expressing Cells.

**(A)** and **(B)** *WUS* expression in wild-type inflorescence SAM is below the outermost three (shown) or two (data not shown) layers.
**(B)** *WUS* expression in the wild-type floral meristem (FM) is below the outermost two layers.
**(C)** *WUS* expression in the *clv3-2* inflorescence SAM concentrates in the cells below the L2 layer and at lower level in the L2 layer.
**(D)** *WUS* expression in the *clv3-2* floral meristem expands into the L2 layer.
**(E)** and **(G)** *WUS* expression in most of the *han-1* inflorescence SAMs is diffuse.
**(F)** and **(H)** *WUS* expression in the *han-1* floral meristems is shifted to include the L2 and L1 layers.
**(I)** *WUS* expression in the *han-1 clv3-2* double mutant inflorescence SAM is concentrated in the L2 layer.
**(J)** *WUS* expression in the *han-1 clv3-2* double mutant floral meristem extends in some cases into the L1 layer.
**(K)** Overview of a *clv3-2* inflorescence SAM.
**(L)** Partial view of a *han-1 clv3-2* double mutant inflorescence SAM.
Bars = 50 μm.

To find out how early the aberrant *WUS* expression occurs in *han* mutants, as well as how early its impact on morphological development is manifested, embryos from *han-1*/+ siliques were examined. Morphological defects can be observed as early as globular stage, when the shapes of what are likely the *han-1* mutant embryos deviate from the wild type (Figures 6A and 6B). By the heart stage, some mutant embryos clearly fail to properly develop cotyledons, which appear as small stubs (Figure 6D) or are barely visible (data not shown). By the torpedo or walking stick stages, mutant embryos appear stunted to various degrees, with a majority having thickened hypocotyls and small cotyledons in numbers ranging from two to four (Figures 6F and 6H).

In wild-type embryos, *WUS* is expressed in the center two cells at the subepidermal layer of the apical region at the globular and transition stages (Figure 6I). At the heart stage, *WUS* expression shifts to the central two cells of the corpus (Figure 6K). In mature embryos, *WUS* is expressed even deeper in the meristem and is excluded from the L2 layer (Figure 6M). However, in apparent *han* mutant embryos, *WUS* expression is observed in both L2 and corpus cells and in more than two cells in the transition stage embryo, which corresponds to the enlarged size of the embryo (Figure 6J). At the heart stage, *WUS* expression is likewise concentrated in both L2 cells and deeper cells (Figure 6L). By the walking stick stage, expression in some apparent *han-1* embryos stays strong in L2 cells (Figures 6N to 6P). Aberrant *WUS* expression in early stage *han* embryos suggests that HAN is normally required to control the number of *WUS* expressing cells and to correctly position these cells.

Because there is a feedback loop interaction between WUS and CLV3 in shoot and floral meristems (Brand et al., 2000; Schoof et al., 2000), we also examined *CLV3* expression in *han* mutants in both embryonic and inflorescence stages. No obvious difference in *CLV3* expression was observed between *han* mutant and wild-type plants during embryogenesis, but *CLV3* expression becomes variable in *han* inflorescence meristems (Figure 7). In approximately half of the cases, *CLV3* expression appears fairly normal as compared with the wild type (Figures 7C and 7D versus 7A and 7B). However, in the other half of the cases, *CLV3* expression becomes slightly (Figure 7E, arrow) or more widely diffuse (Figures 7F to 7H, arrows). The effect of *han* on the *CLV3* expression domain could be because of the alteration of the *WUS* expression domain that occurs in early embryogenesis before *CLV3* expression is initiated.

### Interactions between HAN and the CLV Pathway

To uncover potential regulatory interactions between HAN and CLV, we also examined *HAN* expression in *clv3-2* mutants. The *HAN* expression pattern in *clv3-2* was unchanged in all tissues except for the meristems, where *HAN* was detected strongly in the L2 and corpus layers along the entire fasciated SAM as well as in the late stage floral meristems (Figures 8A, arrowheads, 8B, large arrow). This expression pattern mimicked the *WUS* expression pattern in *clv3-2* mutants (Figure 8C, arrowhead, 8D, large arrow), suggesting that in the absence of CLV3 activity, *HAN* expression is ectopically induced in the apical region of the SAM. Because *WUS* is also ectopically expressed in *clv1* mutants (Schoof et al., 2000), we also assessed whether *HAN* expression was altered in *clv1* mutants. *HAN* shows a similar expression pattern in the SAM of *clv1-4* mutants as in *clv3-2* (data not shown). However, *HAN* is not ectopically expressed in the *clv2-1* SAM (data not shown). To find out how early *HAN* expression is perturbed, we examined *HAN* expression in *clv3-2* embryos. From globular stage to mature embryos, the *HAN* expression is similar in wild-type and *clv3-2* mutants (Figures 8E to 8G). This suggests that *HAN* expression is altered in the *clv3-2* SAM during postembryonic development.

### Phenotypes Caused by Ectopic Expression of *HAN*

To examine the effects of HAN gain-of-function, we generated transgenic plants carrying *35S*:*HAN* or *35S*:*HAN-GR* (glucocorticoid receptor binding domain; Lloyd et al., 1994) transgenes. Among Landsberg *erecta* (L*er*) plants transformed with a *35S*:*HAN* construct, only four T1 transgenic plants were produced from >4 mL ($\sim 1.5 \times 10^4$) of seeds screened, which is substantially lower than the normal transformation efficiency for the binary vector used (>0.05%). Of the four, one looked fairly normal, but the others were small in size, with unevenly shaped rosette leaves and cauline leaves that gradually turned purple, starting from the abaxial side (Figure 9A). The smallest one of the three died prematurely after making some miniature flowers that did not produce seeds. The remaining two plants had smaller inflorescences than the wild type (Figures 9B and 9C). Floral organs were shorter in length when compared with the wild type at similar stages. The gynoecium was short and also appeared bulky, with wavy surfaces and elongated peduncles compared with the wild type (Figures 9D and 9E). The scarcity of T1 transformants suggests that constitutive overexpression of *HAN* might be deleterious.

More than 50 T1 *35S*:*HAN-GR* transgenic plants were generated and all looked normal in the absence of dexamethasone (DEX). When treated three times at 1-d intervals with 10 μM DEX solution, the transgenic plants showed a distinctive morphology. Young flowers opened up precociously (Figure 9F), and stem elongation was retarded. In the 2-d interval between the 2nd and 3rd treatments, the mock-treated control plants increased in height an average of 2.1 cm, whereas the DEX-treated transgenic plants only increased an average of 0.8 cm. When seedlings from a homozygous T2 line were treated with 10 μM DEX four times at 1-d intervals, starting on postgermination day 11 (solution applied via soil), plants began to show accelerated leaf senescence after the second treatment. New leaves were still produced, but leaf expansion was inhibited, and leaf blades were serrated, similar to the leaves of the *35S*:*HAN* transgenic lines (Figure 9H, arrow). Twelve days after the last treatment, the mock-treated control group plants had already bolted (Figure 9G), but approximately half of the DEX-treated plants were dead, and the surviving plants remained in miniature form (Figure 9H). The miniature plants were still able to produce flowers that grew extremely slowly and never reached normal size. These flowers had normal organ identities and numbers but were male sterile. When seeds from a T2 homozygous line were germinated on DEX plates, all seedlings ceased growth at the stage shown in Figure 9I and did not develop further. Transgenic seedlings on non-DEX MS plates

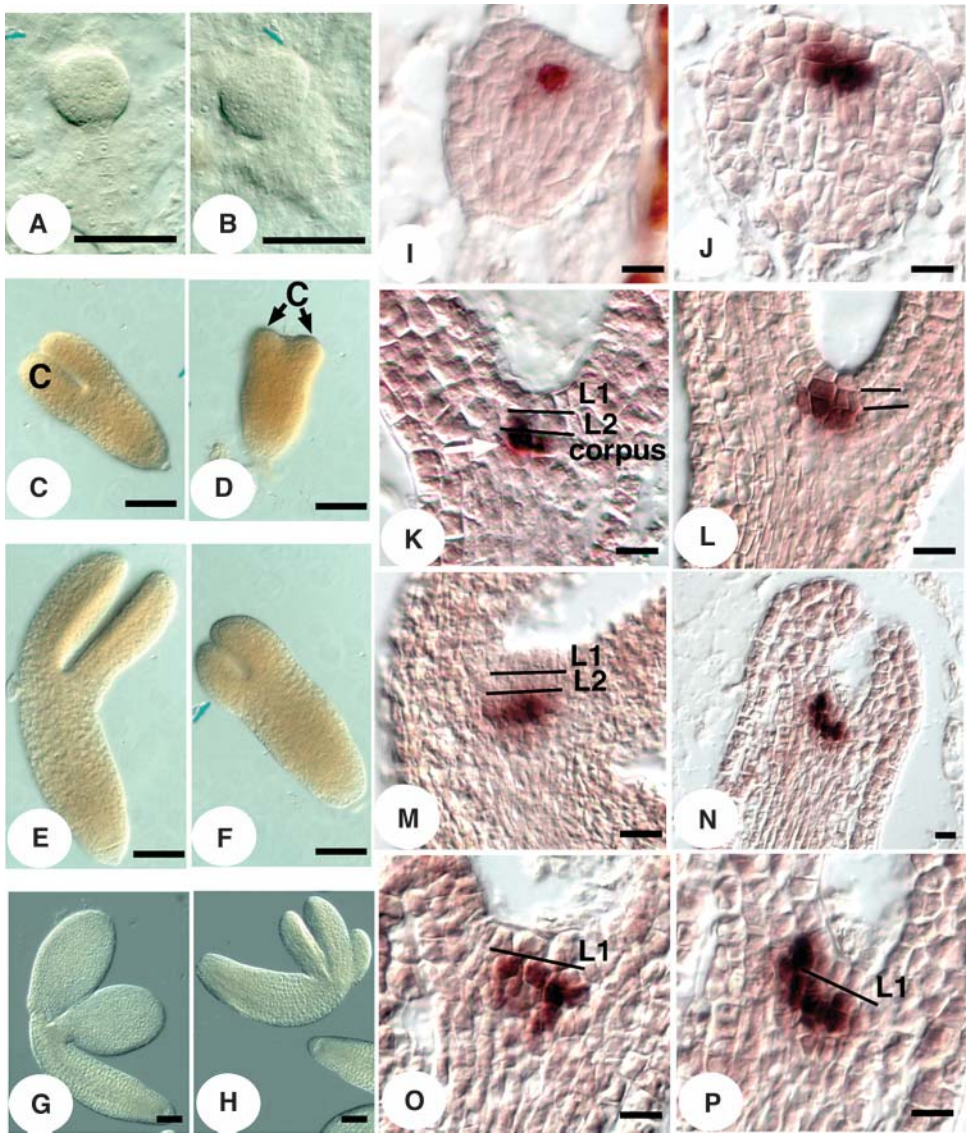


**Figure 6.** *han* Mutant Embryo Defects and Perturbed *WUS* Expression in *han* Embryos.

**(A)** Globular stage wild-type embryo.
**(B)** Globular stage *han-1* mutant embryo.
**(C)** Late heart stage wild-type embryo. C, cotyledon.
**(D)** Late heart stage *han-1* embryo with stunted cotyledons.
**(E)** Walking stick stage wild-type embryo.
**(F)** Walking stick stage *han-1* embryo.
**(G)** Mature wild-type embryo.
**(H)** Mature *han-1* mutant embryo with three cotyledons.
**(I)** *WUS* expression in the transition stage wild-type embryo is concentrated in two cells in the subepidermal L2 layer.
**(J)** *WUS* expression in the transition stage *han-1* embryo is located in more than two cells within and beneath the L2 layer.
**(K)** *WUS* expression in the heart stage wild-type embryo is shifted to two central cells in the corpus.
**(L)** *WUS* expression in the heart stage *han-1* embryo in the L2 layer.
**(M)** *WUS* expression in the mature stage wild-type embryo is centered below the outermost two layers.
**(N)** *WUS* expression in the mature *han-1* embryo.
**(O)** and **(P)** *WUS* expression in the L2 layer of mature *han-1* embryos. **(P)** is an enlarged view of **(N)**.
Bars = 50 μm in **(A)** to **(H)** and 10 μm in **(I)** to **(P)**.

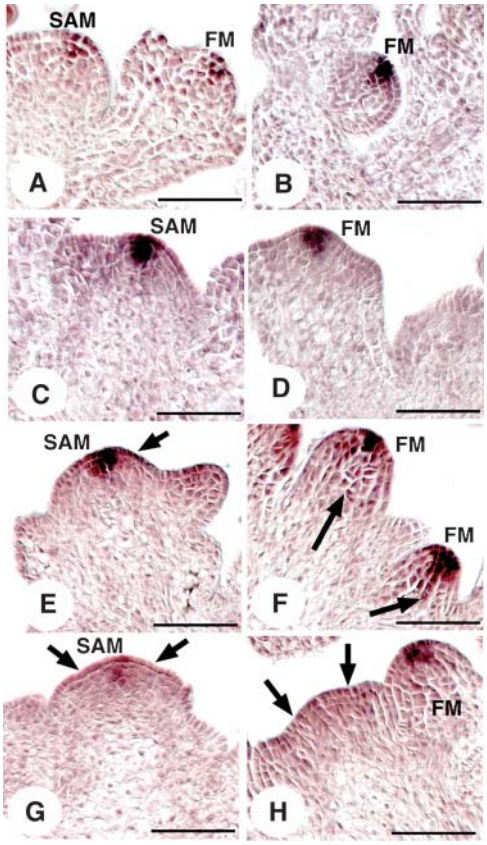


**Figure 7.** *CLV3* Expression in *han* Mutants.

**(A)** and **(B)** *CLV3* expression in the wild-type inflorescence SAM and floral meristem (FM) is concentrated in the central outermost three layers, at about three to four cells width.
**(C)** and **(D)** *CLV3* expression appears fairly normal in some *han* inflorescence SAMs and floral meristems.
**(E)** *CLV3* expression is slightly diffuse in some *han* mutants.
**(F)** *CLV3* expression is expanded in some *han* floral meristems.
**(G)** and **(H)** *CLV3* expression is markedly diffuse in some *han* mutants. Arrows point to the regions of diffuse expression.
Bars = 50 μm.

grew normally, as did wild-type seedlings on DEX and non-DEX plates.

Stalled growth in *35S:HAN-GR* DEX-treated transgenic seedlings suggests inhibited cell proliferation/growth and possible cessation of shoot and root meristem activity. To evaluate this, the SAM structures of homozygous *35S:HAN-GR* seedlings that were germinated on either DEX or non-DEX plates were examined on postgermination day 10 using scanning electron microscopy. Whereas the non-DEX-treated control SAMs were dome-shaped like wild-type SAMs (Figure 9J), the DEX-treated SAMs either were flat (Figure 9K, arrow) or were no longer identifiable between the leaf primordia (Figure 9L, arrow). Because *WUS* serves as a marker of active meristematic cell activity in the SAM during normal development, we examined *WUS* expression in day 10 plants as well as in day 6 seedlings germinated on DEX plates. In both cases, no *WUS* expression was found in the DEX-treated seedlings (Figure 9N), suggesting that they had already lost active SAM activity. Similarly, *STM* expression is also lost in treated seedlings by day 6 (data not shown). *HAN* expression in the same plants was strong and ubiquitous (data not shown). DEX-treated *35S:HAN-GR* seedlings had smaller cells in all cell layers of the cotyledons compared with untreated ones (data not shown), which explains at least in part why the treated plants have small cotyledon blades. In addition, stomatal pores in the cotyledons of induced seedlings were often composed of three or more guard cells instead of two cells as in the control (Figures 9O to 9Q), implying abnormal cell division of the guard cell mother cells or incomplete differentiation of the guard cells. In contrast with the cotyledon cells, the root cells of the induced seedlings were in general larger in size than those of the control group (Figures 9R and 9S). Additionally, in the induced roots, cell files were not as organized as in the control, and root caps were usually

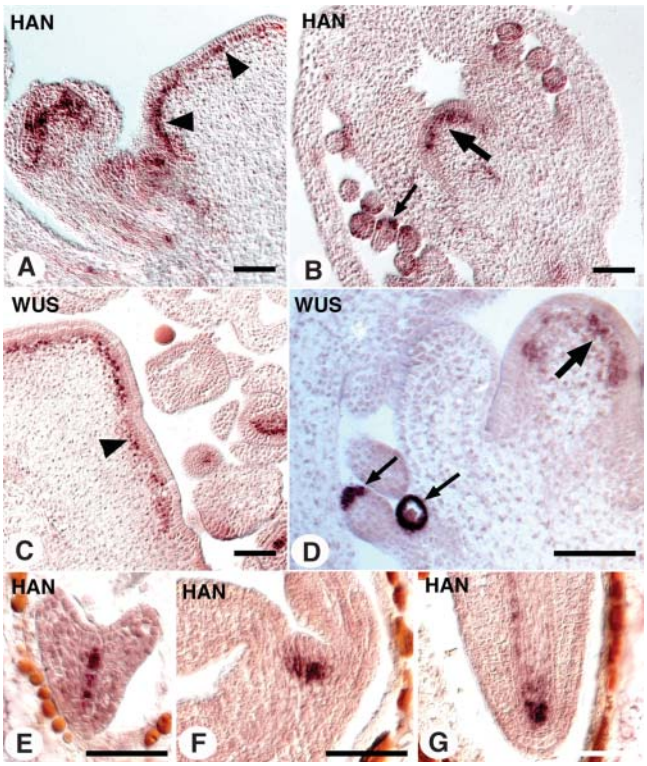


**Figure 8.** *HAN* Is Ectopically Expressed in *clv3-2* Mutants.

**(A)** *HAN* expression in a *clv3-2* inflorescence SAM (arrowheads).
**(B)** *HAN* expression in the undifferentiated center dome cells in a late stage *clv3-2* flower (large arrow). Small arrow points to *HAN* expression in the integuments of ovule.
**(C)** *WUS* expression in a *clv3-2* inflorescence SAM (arrowhead).
**(D)** *WUS* expression in the undifferentiated cells in a late stage *clv3-2* flower (large arrow). Small arrows point to *WUS* expression in the nucellus.
**(E)** *HAN* expression in a heart stage *clv3-2* embryo.
**(F)** and **(G)** *HAN* expression in the SAM and the root of a *clv3-2* embryo in late torpedo stage, respectively.
Bars = 50 μm.

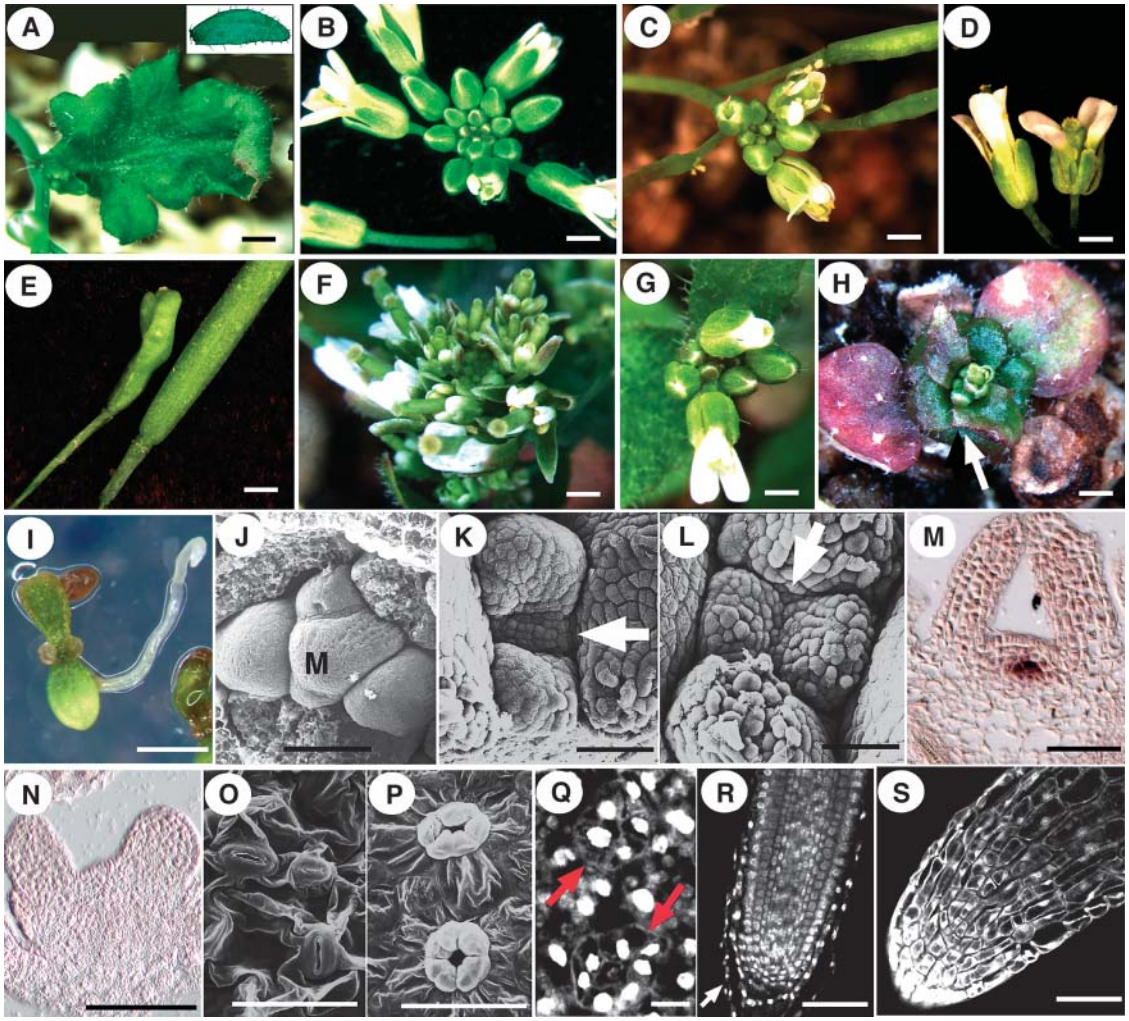


**Figure 9.** Phenotypes of Ectopic *HAN* Expression.

**(A)** Lobed cauline leaf from a *35S*:*HAN* plant. Inset shows a wild-type cauline leaf.
**(B)** Wild-type inflorescence.
**(C)** *35S*:*HAN* inflorescence.
**(D)** Wild-type (left) and *35S*:*HAN* flowers.
**(E)** Wild-type (right) and *35S*:*HAN* siliques.
**(F)** to **(H)** *35S*:*HAN-GR* transformants.
**(F)** DEX-treated inflorescence has early opening flowers and a short stem.
**(G)** Seedlings mock-treated from at 11 d of age, shown at 29 d old.
**(H)** Seedlings treated with DEX beginning at 11 d of age, shown at 29 d old. Arrow points to lobed leaf margins.
**(I)** Homozygous *35S*:*HAN-GR* seedling germinated on a DEX plate at 9 d.
**(J)** SAM of 10-d-old wild-type seedling. M, SAM.
**(K)** and **(L)** SAMs of 10-d-old *35S*:*HAN-GR* seedlings germinated on DEX plates. Arrows point to the SAMs.
**(M)** *WUS* expression in a 10-d-old *35S*:*HAN-GR* seedling germinated on non-DEX plates.
**(N)** Absence of *WUS* expression in a 10-d-old *35S*:*HAN-GR* seedling germinated on DEX plates.
**(O)** Non-DEX-induced control stomata with two guard cells.
**(P)** and **(Q)** Guard cells in 10-d-old and 6-d-old DEX-treated *35S*:*HAN-GR* seedlings, respectively. Arrows point to stomata with five or seven guard cells.
**(R)** Mock-treated *35S*:*HAN-GR* root tip. Arrow points to the root cap.
**(S)** DEX-induced *35S*:*HAN-GR* root tip.
Bars in **(A)** to **(I)** = 1 mm; bars in **(J)** to **(S)** = 50 μm (except for **[Q]**, in which the bar = 10 μm).

diminished or absent, further indicating aberrant cell division and positioning in *HAN*-overexpressing plants.

## DISCUSSION

### Functions of HAN in Flower Development

*HAN* mutations affect various aspects of flower development, including floral meristem size, floral organ separation, floral organ number and size, and floral organ identity. This indicates that HAN plays multiple developmental roles. Because the floral meristem size reduction precedes the other floral organ defects, it could be the primary cause of the other defects. Reduced floral meristem size suggests that HAN is important for controlling the proliferation of floral meristem cells, which are embraced by the cup-shaped *HAN* expression domain. *WUS* expression is more diffuse in *han* floral meristems than in the wild type, and it could be that a centered and high level of *WUS* expression, mediated by *HAN*, is required for promoting floral meristem cell proliferation. In addition, ectopic *WUS* expression in peripheral zone cells could hinder their progression toward cell differentiation and therefore repress organ primordium initiation. This might explain why floral organ initiation in *han* floral meristems is delayed. On the other hand, because the level of ectopic *WUS* expression in these cells is low, the peripheral zone cells may not be able to be transformed into central zone cells and thus do not contribute to a larger floral meristem. An alternative explanation for the reduced floral meristem size is that, as *HAN* is expressed in cells appearing to be the provascular tissue cells in as early as stage 1 flowers, the *HAN*-expressing cells may serve to transport nutrients or signals from other parts of the plant to the developing flower. In the case of insufficient supply of these factors, growth of the floral meristem is hindered.

However, unlike in SAM development where *han* mutations interact synergistically with *clv* mutations (see below), *han* appears epistatic to *clv* in flower development. *han clv* double mutants have similar or greater loss of floral organs than *han* single mutants, indicating that the mode of action of the HAN protein in controlling the proliferation of floral meristem cells may be different from that in the SAM, or HAN may have additional functions in flower development. The difference between HAN function in the development of SAM and flower is also reflected by the observation that *wus* is epistatic to *han* in SAM development but not in flower development in *wus*/*wus han-1*/+ mutants because these have reduced floral organ numbers compared with *wus* single mutants. This suggests that *HAN* is required for initiating and/or maintaining the proliferation of floral meristematic cells in *wus* mutants. By contrast, the increased leaf-like or shoot-like organs arising from the axils of leaves in *wus han* double mutants compared with *wus* single mutants suggests that HAN restricts meristematic cell activity in axillary meristem positions.

In addition to controlling floral meristem cell proliferation, HAN also appears to act in establishing boundaries between different whorls, as well as between different organ primordia in the same whorl. One possible mechanism for the boundary establishment is that HAN prevents cells expressing it from dividing, leading to the gap between organ primordia. In *han* mutants, gaps fail to form or be maintained, therefore resulting in one of its major floral defects: organ fusions. This theory is supported by the observation that overexpression of *HAN* causes growth retardation, small organs, and abolished meristem activity.

The other major floral defect in *han* mutants is decreased organ numbers in all four whorls, particularly in the 2nd and 3rd whorls. This could be a consequence of either reduced floral meristem size preceding organ initiation, diminished boundary formation, or both.

### Interactions between HAN and the CLV-WUS Pathway in SAM Development

The *HAN* expression domain overlaps with the *WUS* expression domain during embryonic development, but *HAN*-expressing cells surround *WUS*-expressing cells in mature SAMs, with the possibility of some overlap. This suggests that, as in flower development, HAN's function in the SAM is to set up a boundary between the meristem and nascent organ primordia, which is required to confine *WUS*-expressing cells to a central domain. The *WUS* expression domain is spatially perturbed in *han* mutants beginning early in embryogenesis, before *CLV3* and *CLV1* expression initiates. This is consistent with the loss of *WUS RNA* in *HAN* overexpression.

Mutations in *HAN* greatly enhance *clv* phenotypes, implying that HAN may normally function to limit SAM size. Several mutations have been shown to enhance *clv* mutant phenotypes, including *wiggum/enhanced response to abscisic acid1* and *ultrapetala* (Running et al., 1998; Fletcher, 2001). However, unlike the other enhancers, *han* loss of function does not lead to a SAM fasciation phenotype. Rather, some *han* mutants show flat or smaller SAMs toward the late stage of flowering. So how might perturbed *WUS* expression be tied to gradually flattened and reduced size of the SAM in *han* mutants? It is possible that diffuse *WUS* expression might result in a low level of WUS activity in individual cells, causing meristem cells gradually to lose their potency as stem cells, which may lead to flat and smaller SAMs. This possibility is supported by the observation that in some *han* inflorescence SAMs, the *CLV3* domain also appears diffuse, which could have resulted from the low level of *WUS* expression. In contrast with *han* mutants, *clv* mutants have an expanded domain of *WUS* expression as a result of SAM enlargement. The different phenotypes of *han* and *clv* SAMs may be attributable to the fact that in the latter, *WUS* expression is not diffuse but is located in two cell layers below the epidermal cells of the SAM, and the expression level is fairly uniform across a single layer. Therefore, the mechanisms through which HAN and CLV control *WUS*-expressing cells are likely different. In either case, it is not clear whether the expanded *WUS* expression is caused by enhanced proliferation of *WUS*-expressing cells or by peripheral zone cells activating *WUS* expression.

Why then might the perturbed *WUS* expression in *han* mutants greatly enhance SAM fasciation in *clv* mutants? As mentioned above, HAN may play a partially CLV-independent role in restricting *WUS* expression to the L3 layer. A combination of *han* and *clv* mutations could lead to more *WUS*-expressing cells in the outer cell layers and peripheral zone, as well as increased levels of *WUS* expression, thus causing the formation of a more fasciated meristem. Although the above scenario may account

for the increased SAM fasciation in *han*/*clv* double mutants, we cannot exclude the possibility that organ differentiation is further delayed in *han*/*clv* than in *han* mutants, which might also contribute to the accumulation of SAM cells.

The size variation of *han* mutant SAMs at different stages, as well as the variation of *WUS* and *CLV3* expression in different *han* mutant meristems, suggests that the structure of the *han* SAM is dynamic and possibly self-correcting. Nevertheless, a more precise genetic control is required for a wild-type SAM, as *han* mutant SAMs become more irregularly shaped and produce more deformed organ primordia toward the later stages of development. The dynamic aspect of the SAM is shown by the observation that the *WUS* expression domain in wild-type inflorescence SAMs is variable either beneath two cell layers or (more often) three cell layers, suggesting that the *WUS* expression domain is fluctuating within an individual SAM during normal development. Another indication of regulatory activity in the SAM is the observation that in *clv* embryos, *WUS* expression is shifted to the L2 layer at the heart stage but moves to the layers underneath the L2 in mature embryos (Schoof et al., 2000). After postembryonic development, the *WUS* domain shifts back to include the L2 layer in *clv* inflorescence SAMs. We can speculate that in *han* mutants, the dynamics of *WUS*-expressing cells are imprecise, leading to a gradual disruption of the SAM structure.

In both *clv1* and *clv3* mutants, *HAN* expression is elevated and expanded along the fasciated SAM, overlapping with the *WUS* expression domain. Because *HAN* expression is not changed during *clv3* mutant embryogenesis, the alteration of the *HAN* domain happens during postembryonic development. Is there any biological function of *HAN* expression in the outer layers of the SAMs in *clv3* and *clv1* mutants, or is it a mere effect of the altered SAM structure, causing the *han* domain to stretch laterally? It is possible that ectopic *HAN* expression in *clv3* SAMs prevents *WUS* from further shifting toward the L2/L1 layer, making it still concentrated in the layer below the L2 layer. This explains why in the absence of both CLV and HAN functions, *WUS* becomes concentrated in the L2 layer and sometimes even shifted to the L1 layer. It is worth noting that *HAN* expression remains fairly normal in *clv3* mutant flowers, further indicating that the mode of action of HAN in the floral meristem might be different from that in the SAM.

### Effect of Differentiating Tissues on SAM Development

*HAN* is expressed in the provascular tissues below the *WUS* domain and begins to overlap with the *WUS* domain during the transition to the walking stick stage of embryogenesis. Later in the adult SAM, *HAN* expression marks the boundaries between the meristem and its initiating organs and between the *WUS* domain and the differentiated stem tissues below, with overlap between the *HAN* and *WUS* expression domains not being excluded. The effect of HAN on *WUS*-expressing cells could be direct during embryogenesis, but during postembryonic development it seems likely to be non-cell-autonomous. This adds another example of more mature cells exerting effects on meristematic cell activities (Stuurman et al., 2002). One can speculate that *HAN*-expressing cells could express certain secreted factor(s) or that the HAN protein could move from cell to cell via plasmodesmata to coordinate cell division/differentiation activity of *WUS*-expressing cells or to prevent non-*WUS*-expressing cells from activating *WUS*. In the absence of this coordination or prevention, cell division and differentiation become aberrant.

The *han* mutant phenotypes, *HAN* expression patterns, meristem marker analysis in *han* mutants, and overexpression of *HAN* all suggest that HAN is involved in regulating meristem cell activity by setting up a boundary between the meristem and differentiating organ primordia. In the event of HAN loss of function, the meristematic structure becomes disorganized, leading to meristem size reduction, reduced organ numbers and size, and organ fusion. Further molecular and biochemical studies will shed light on the mechanisms through which HAN regulates these important developmental processes.

## METHODS

### Plant Growth

Seeds were imbibed at 4°C cold room for 4 d before growth in constant light at 22°C. Plant age is calculated from the first day at 22°C. Seeds germinated on MS plates were sterilized as described at http://plantpath.wisc.edu/~afb/vapster.html.

### Isolation of *han* Alleles and Mapping of *han* Mutation

The *han-1* allele (Clark et al., 1994) was isolated during T-DNA transformation mutagenesis of Wassilewskija ecotype seeds. The *han-2* allele was isolated from an ethyl methanesulfonate mutagenesis screen in Landsberg *erecta* (L*er*). The *han-3* and *han-4* alleles were both isolated from an activation-tagging screen in the *clv1-1* mutant background (Weigel et al., 2000). Each single *han* mutant was backcrossed to L*er* three times before phenotypic and genetic characterization.

The *HAN* gene was positionally mapped by crossing the *han-1* mutant to the wild-type Columbia strain. DNA was prepared from 423 *han-1* mutant plants in the T2 generation. Using cleaved amplified polymorphic sequence markers, recombination events between *han-1* and surrounding regions were identified (Konieczny and Ausubel, 1993). Using this approach, the *HAN* region was narrowed down to BAC clone ATF18B3 on chromosome 3 (information about the polymorphic markers spanning *HAN* region is available in the supplemental data online). Sequencing of candidate genes revealed a 3262-bp DNA deletion at At3g50870 gene locus in *han-1*, when compared with wild-type sequences.

### Morphological Analyses

Scanning electron microscope images were generated as described (Bowman et al., 1989). Confocal laser scanning microscopy images were generated as described (Running et al., 1995).

For 4′,6-diamidino-2-phenylindole staining, samples were fixed in ethanol/acetic acid (3:1) for 4 h on ice, washed twice in PBT (1× PBS with 0.1% Tween-20), each for 45 min, then stained with 1 μg/mL of 4′,6-diamidino-2-phenylindole in PBT for 15 min at room temperature. Samples were then rinsed four times with PBT and once with 25% glycerol. They were mounted on depression slides with glycerol and observed with a Zeiss LSM 510 META NLO confocal microscope (Jena, Germany) using a Chameleon titanium-sapphire laser at a wavelength of 760 nm.

### In Situ Hybridization

*HAN* expression was examined by in situ hybridization using a full-length *cDNA* probe. The results were also confirmed using a 620-bp *HAN* DNA

fragment starting from 170 bp upstream of the start codon and ending before the zinc finger domain (data not shown). Both *HAN* probes were tested on *han-1* mutant samples and did not detect any specific signals. *WUS*, *CLV3*, and *CLV1* probes were generated as described previously (Clark et al., 1997; Mayer et al., 1998; Brand et al., 2000). Apparent *han-1* embryos were determined by the deviation of their morphology from the wild type in serial sections. For *WUS* and *CLV3* probes, sections of the wild type and *han* mutant inflorescences were hybridized on the same slides or on different slides but were paired in sandwiches during probe hybridization, antibody incubation, and antibody detection. Conditions for all slides were identical in the remaining procedures. In situ hybridization was done by following the protocol at http://www.its.caltech.edu/~plantlab/html/protocols.html with the following modifications. (1) After antibody reaction followed by four washes with antibody buffer, slides were equilibrated in detection buffer for 10 min (100 mM Tris-HCl, pH 9, 100 mM NaCl, and 50 mM $MgCl_2$). Excess detection buffer was blotted off, and slides were then incubated with substrate solution (0.2 mM 5-bromo-4-chloro-3-indolyl phosphate and 0.2 mM nitro blue tetrazolium in detection buffer with 10% [w/v] polyvinyl alcohol [70 kD]) for 12 to 24 h at 30°C in darkness. (2) Slides were rinsed three times in distilled water to stop the detection reaction and mounted with 50% glycerol for observation under the microscope.

### Construction of *35S:HAN* and *35S:HAN-GR* Lines

Both constructs were generated using the pGreen 0229 vector containing a 2× *35S* promoter and a *nopaline synthase* terminator (http://www.pgreen.ac.uk/JIT/pGreen0000_fr.htm). Transformation was performed in L*er* plants (see protocol at http://plantpath.wisc.edu/~afb/protocol.html from Andrew Bent's lab in University of Illinois at Urbana-Champaign).

### DEX Solution and Mock Solution

DEX stock solution (10 mM in ethanol) was stored at −20°C for up to 2 weeks. DEX solution (10 mM) was made by diluting the stock solution in pure water with or without 0.01% Triton X-100 (for inflorescences or soil, respectively). Mock solution consists of an equal concentration of ethanol and Triton X-100 in water per the final DEX solution.

## ACKNOWLEDGMENTS

We thank Ken Feldmann for allowing us to screen his *T-DNA* population, which resulted in the isolation of *han-1*, and Steven Clark for providing us with the *han-2* allele. We also thank our laboratory colleagues and Robert Williams for their critical reading of the manuscript. This project is sponsored by National Science Foundation Grant IBN-0211670 to E.M.M.

Received June 2, 2004; accepted July 10, 2004.

## REFERENCES

**Aida, M., Ishida, T., and Tasaka, M.** (1999). Shoot apical meristem and cotyledon formation during Arabidopsis embryogenesis: Interaction among the CUP-SHAPED COTYLEDON and SHOOT MERISTEMLESS genes. Development **126,** 1563–1570.

**Bowman, J.L., Smyth, D.R., and Meyerowitz, E.M.** (1989). Genes directing flower development in Arabidopsis. Plant Cell **1,** 37–52.

**Brand, U., Fletcher, J.C., Hobe, M., Meyerowitz, E.M., and Simon, R.** (2000). Dependence of stem cell fate in Arabidopsis on a feedback loop regulated by CLV3 activity. Science **289,** 617–619.

**Byrne, M.E., Barley, R., Curtis, M., Arroyo, J.M., Dunham, M., Hudson, A., and Martienssen, R.A.** (2000). Asymmetric leaves1 mediates leaf patterning and stem cell function in Arabidopsis. Nature **408,** 967–971.

**Clark, S.E., Jacobsen, S.E., Levin, J.Z., and Meyerowitz, E.M.** (1996). The CLAVATA and SHOOT MERISTEMLESS loci competitively regulate meristem activity in Arabidopsis. Development **122,** 1567–1575.

**Clark, S.E., Sakai, H., and Meyerowitz, E.M.** (1994). Inflorescence development in clavata mutants. In Arabidopsis: An Atlas of Morphology and Development, J.L. Bowman, ed (New York: Springer-Verlag), pp. 214–215.

**Clark, S.E., Williams, R.W., and Meyerowitz, E.M.** (1997). The CLAVATA1 gene encodes a putative receptor kinase that controls shoot and floral meristem size in Arabidopsis. Cell **89,** 575–585.

**Fletcher, J.C.** (2001). The ULTRAPETALA gene controls shoot and floral meristem size in Arabidopsis. Development **128,** 1323–1333.

**Fletcher, J.C., Brand, U., Running, M.P., Simon, R., and Meyerowitz, E.M.** (1999). Signaling of cell fate decisions by CLAVATA3 in Arabidopsis shoot meristems. Science **283,** 1911–1914.

**Fletcher, J.C., and Meyerowitz, E.M.** (2000). Cell signaling within the shoot meristem. Curr. Opin. Plant Biol. **3,** 23–30.

**Gallois, J.L., Woodward, C., Reddy, G.V., and Sablowski, R.** (2002). Combined SHOOT MERISTEMLESS and WUSCHEL trigger ectopic organogenesis in Arabidopsis. Development **129,** 3207–3217.

**Kayes, J.M., and Clark, S.E.** (1998). CLAVATA2, a regulator of meristem and organ development in Arabidopsis. Development **125,** 3843–3851.

**Konieczny, A., and Ausubel, F.M.** (1993). A procedure for mapping Arabidopsis mutations using co-dominant ecotype-specific PCR-based markers. Plant J. **4,** 403–410.

**Laux, T., Mayer, K.F., Berger, J., and Jurgens, G.** (1996). The WUSCHEL gene is required for shoot and floral meristem integrity in Arabidopsis. Development **122,** 87–96.

**Lenhard, M., Jurgens, G., and Laux, T.** (2002). The WUSCHEL and SHOOTMERISTEMLESS genes fulfil complementary roles in Arabidopsis shoot meristem regulation. Development **129,** 3195–3206.

**Lloyd, A.M., Schena, M., Walbot, V., and Davis, R.W.** (1994). Epidermal cell fate determination in Arabidopsis: Patterns defined by a steroid-inducible regulator. Science **266,** 436–439.

**Long, J.A., Moan, E.I., Medford, J.I., and Barton, M.K.** (1996). A member of the KNOTTED class of homeodomain proteins encoded by the STM gene of Arabidopsis. Nature **379,** 66–69.

**Mayer, K.F., Schoof, H., Haecker, A., Lenhard, M., Jurgens, G., and Laux, T.** (1998). Role of WUSCHEL in regulating stem cell fate in the Arabidopsis shoot meristem. Cell **95,** 805–815.

**McConnell, J.R., and Barton, M.K.** (1998). Leaf polarity and meristem formation in Arabidopsis. Development **125,** 2935–2942.

**Rojo, E., Sharma, V.K., Kovaleva, V., Raikhel, N.V., and Fletcher, J.C.** (2002). CLV3 is localized to the extracellular space, where it activates the Arabidopsis CLAVATA stem cell signaling pathway. Plant Cell **14,** 969–977.

**Running, M.P., Clark, S.E., and Meyerowitz, E.M.** (1995). Confocal microscopy of the shoot apex. Methods Cell Biol. **49,** 217–229.

**Running, M.P., Fletcher, J.C., and Meyerowitz, E.M.** (1998). The WIGGUM gene is required for proper regulation of floral meristem size in Arabidopsis. Development **125,** 2545–2553.

**Schoof, H., Lenhard, M., Haecker, A., Mayer, K.F., Jurgens, G., and Laux, T.** (2000). The stem cell population of Arabidopsis shoot meristems in maintained by a regulatory loop between the CLAVATA and WUSCHEL genes. Cell **100,** 635–644.

**Smyth, D.R., Bowman, J.L., and Meyerowitz, E.M.** (1990). Early flower development in Arabidopsis. Plant Cell **2,** 755–767.

**Souer, E., van Houwelingen, A., Kloos, D., Mol, J., and Koes, R.** (1996). The no apical meristem gene of Petunia is required for pattern formation in embryos and flowers and is expressed at meristem and primordia boundaries. Cell **85,** 159–170.

**Stuurman, J., Jaggi, F., and Kuhlemeier, C.** (2002). Shoot meristem maintenance is controlled by a GRAS-gene mediated signal from differentiating cells. Genes Dev. **16,** 2213–2218.

**Takada, S., Hibara, K., Ishida, T., and Tasaka, M.** (2001). The CUP-SHAPED COTYLEDON1 gene of Arabidopsis regulates shoot apical meristem formation. Development **128,** 1127–1135.

**Venglat, S.P., Dumonceaux, T., Rozwadowski, K., Parnell, L., Babic, V., Keller, W., Martienssen, R., Selvaraj, G., and Datla, R.** (2002). The homeobox gene BREVIPEDICELLUS is a key regulator of inflorescence architecture in Arabidopsis. Proc. Natl. Acad. Sci. USA **99,** 4730–4735.

**Vroemen, C.W., Mordhorst, A.P., Albrecht, C., Kwaaitaal, M.A., and de Vries, S.C.** (2003). The CUP-SHAPED COTYLEDON3 gene is required for boundary and shoot meristem formation in Arabidopsis. Plant Cell **15,** 1563–1577.

**Waites, R., Selvadurai, H.R., Oliver, I.R., and Hudson, A.** (1998). The PHANTASTICA gene encodes a MYB transcription factor involved in growth and dorsoventrality of lateral organs in Antirrhinum. Cell **93,** 779–789.

**Weigel, D., et al.** (2000). Activation tagging in Arabidopsis. Plant Physiol. **122,** 1003–1013.

**Weir, I., Lu, J., Cook, H., Causier, B., Schwarz-Sommer, Z., and Davies, B.** (2004). CUPULIFORMIS establishes lateral organ boundaries in Antirrhinum. Development **131,** 915–922.